J. Chem. Sci. (2020) 132:109
https://doi.org/10.1007/s12039-020-01816-y

REGULAR ARTICLE

Probing the interaction between human serum albumin and the sodium dodecyl sulphate with fluorescence correlation spectroscopy

VAISHALI SAMANT*, ARGHYA DEY and G NARESH PATWARI*
Department of Chemistry, Indian Institute of Technology Bombay, Powai, Mumbai, Maharashtra 400 076, India
E-mail: samantv@gmail.com; naresh@chem.iitb.ac.in

MS received 1 April 2020; revised 10 June 2020; accepted 15 June 2020

Abstract. The denaturation of human serum albumin (HSA) upon interaction with the surfactant sodium dodecyl sulphate (SDS) was examined by measuring the diffusion time of fluorophore (RITC) tagged HSA under near single-molecule conditions using fluorescence correlation spectroscopy. The diffusion time shows four distinct regions as a function of SDS concentration, which corresponds to (I) opening of the tertiary structure, (II) non-specific SDS aggregation, (III) opening of the secondary structure, and (IV) aggregation of SDS around the secondary structure. Diffusion time increases from 383 μs for the free protein to 1002 μs for the SDS bound protein, which leads to an effective increase in the hydrodynamic radius by a factor of about 2.6.

1. Introduction

Interactions of proteins with surfactants have been extensively investigated[1–21] because of their importance in a variety of processes, which include foods and cosmetics,[2] drug delivery,[2] detergents,[2] and several biotechnological processes.[2] The interaction between ionic surfactants, such as sodium dodecyl sulphate (SDS) and two structurally similar, water-soluble serum albumins such as bovine serum albumin (BSA)/human serum albumin (HSA) are often used as models to understand the protein-surfactant interaction.[1–12] The HSA is a single polypeptide chain comprising 585 amino acid residues.[22] The secondary structure of HSA consists of α-helical regions and regions with chaotic packing, while the tertiary structure consists of three almost identical domains connected assembled with unique loop packing.[23] The interaction of surfactants on HSA has been reported earlier and the changes were monitored using intrinsic fluorescence of Trp214 (domain II).[6,7] The fluorescence spectral studies, both in time and energy domain, reveal that interaction of SDS with HSA is SDS concentration dependent.[6–8]

Fluorescence quenching studies of Trp 214 shows four distinct stages of SDS-HSA binding.[4,9] In the first stage tertiary structure of the protein starts opening up due to specific binding between protein and surfactant. This is followed by a non-cooperative binding stage with almost no change in protein structure. In the third phase, once again cooperative binding takes place which opens up the secondary structure of the protein. Further addition of surfactant leads to the formation of protein-bound micelles, popularly known as necklace-bead structure. Interaction of surfactants (SDS and others) with HSA and BSA have also been investigated using several extrinsic fluorescent probes.[9–16] Further, polarity sensitive extrinsic fluorescent probes, such as 3-(dimethylamino)-8,9,10,11-tetrahydro-7H-cyclohepta[a]naphthalen-7-one and 7-(dimethylamino)-2,3-dihydrophenanthren-4(1H)-one, were utilized to understand the changes in the polarity and

*For correspondence

Electronic supplementary material: The online version of this article (https://doi.org/10.1007/s12039-020-01816-y) contains supplementary material, which is available to authorized users.

Published online: 18 August 2020

hydrogen bonding environment due to binding of SDS (0-8 mM) to HSA.[24] Apart from fluorescence spectroscopy, the interaction between SDS and BSA/HSA has also been investigated using isothermal titration calorimetry and several other methods such as small-angle X-ray and neutron scattering, static and dynamic light scatting, circular dichroism and NMR.[11,18–21] All of these ensemble level investigations reveal that the addition of SDS leads to the stepwise uncoiling of HSA takes place and represents the behaviour of different molecules. On the other hand, the thermal and chemical unfolding of the HSA was reported using fluorescence correlation spectroscopy.[25] A question that arises at this point, is whether or not the near single-molecule measurements are in accord with the ensemble measurements. Therefore, to obtain molecular-level insight into the binding of SDS with HSA and consequent SDS concentration-dependent structural changes, we have carried out these binding studies using fluorescence correlation spectroscopic (FCS) technique which has near single-molecule sensitivity.

2. Experimental

FCS is a technique with which analyses the fluctuations in fluorescence intensity within a tiny volume in the order of a few femtoliters.[27,28] The fluorescence signal varies due to the changes in the number or brightness of the fluorophores inside the detection volume, which can be influenced by diffusion/transport in and out of the detection volume, and other photochemical and photophysical processes.[29–42] As a result, FCS can be used to study various parameters like diffusion coefficient, fluorophore concentration, particle size, chemical reactions, conformational changes, binding/unbinding processes, and several others. FCS studies were carried out using a home-built FCS setup. Briefly, the sample was illuminated by 532 nm DPSS laser (Shanghai Dream Lasers Technologies Co. Ltd.). The excitation light was expanded and reflected with a 532 nm dichroic mirror and then made to overfill the back focal plane of the objective lens (OLYMPUS 60X, 1.2 NA, water immersion). The objective lens focuses the light on the sample placed over a stage and the emitted light from the sample is collected by the same objective lens. The emitted light passes through the 532 nm dichroic mirror and an emission filter and is focussed on to a pinhole with a concavo-convex achromatic lens (Thor Labs), which enables light collection in a confocal geometry. A fiber optic cable is used to collect the light from the pinhole which is then relayed to an APD detector (Perkin Elmer). Signal from APD was fed into the correlator card (Model No. FLEX 99 OEM-12D; www.correlator.com) to generate autocorrelation, which is acquired by a program written in LabView.

The fluctuations in the fluorescence intensity can be analysed using an autocorrelation function, $G(t)$

$$G(t) = \frac{\langle \delta F(t+\tau)\delta F(t)\rangle}{\langle F(t)\rangle^2} \tag{1}$$

This equation measures how the average correlation between the fluorescence intensity $F(t)$ at two-time points t and $(t+\tau)$, which falls off as the time interval τ between the two points increases. For normal Brownian diffusion, these intensity autocorrelation curves can be fitted to equation (2) to obtain the diffusion time (τ_D)

$$G(t) = \frac{1}{N}\left[\frac{1}{1+\left(\tau/\tau_D\right)}\right]\left[\frac{1}{1+\left(r/l\right)^2\left(\tau/\tau_D\right)}\right]^{\frac{1}{2}} \tag{2}$$

Here r is transverse radius and l is the longitudinal radius of the ellipsoidal focal volume. From equation (2) it can be realized that $G_0 = 1/N$. Autocorrelation function can also have multiple components, indicating that different processes contribute to the fluorescence signal fluctuation. In such cases, a multi-component fitting equation can be used, and the corresponding equation for a two-component model would be,

$$G(t) = \frac{1}{N_1}\left[\frac{1}{1+\left(\tau/\tau_{D1}\right)}\right]\left[\frac{1}{1+\left(r/l\right)^2\left(\tau/\tau_{D1}\right)}\right]^{\frac{1}{2}} + \frac{1}{N_2}\left[\frac{1}{1+\left(\tau/\tau_{D2}\right)}\right]\left[\frac{1}{1+\left(r/l\right)^2\left(\tau/\tau_{D2}\right)}\right]^{\frac{1}{2}} \tag{3}$$

In the case of multi-component systems fraction, different species present in the solution contribute to the observed G value with $G_1 = 1/N_1$ and $G_2 = 1/N_2$. When all the contributing species have the same brightness then the sum of all the fractions is equal to unity, however, if different species differ in their brightness then the addition of all fractions can be greater than unity.[43] The value of the parameter r/l (ratio of transverse to the longitudinal radius of focal volume) obtained is very small and hence the square of it is negligible and is kept zero for all fittings.

The FCS setup was calibrated using Rhodamine 6G in water at 298 K. The autocorrelation is fitted to

obtain diffusion time (τ_D), and the diffusion coefficient was obtained using equation (2).[35]

$$r^2 = 4D\tau_D \quad (4)$$

Diffusion coefficient 285 $\mu m^2\ s^{-1}$ was obtained by the normal Brownian diffusion by fitting to equation (4), which is in excellent agreement with the value (300 $\mu m^2\ s^{-1}$) reported earlier.[44]

Fatty acid-free HSA (Sigma-Aldrich) was tagged with RITC (Sigma-Aldrich). For tagging, HSA solution was prepared in pH 8.4 buffer and RITC solution was prepared in spectroscopic grade methanol. Both solutions were mixed with protein: dye concentration 4:1 and stirred for 6 h at room temperature. This solution was directly used for further dilutions. The final concentration of RITC was around 5 nM and that of protein was around 25 nM. SDS (Sigma-Aldrich) Rhodamine 6G (Rh6G; Radiant dyes, Germany) were used as obtained without further purification. For each set of experiments, five different sets of solutions were prepared and a minimum of three autocorrelations curves are recorded for each solution.

3. Results and Discussion

The autocorrelation traces for RITC and RITC tagged HSA are shown in Figure 1. The autocorrelation curve of RITC could be fitted to a single component diffusion model with a diffusion time of 56 μs. The autocorrelation trace for the RITC tagged HSA was fitted to a two-component model with τ_D of the first component fixed at 56 μs. This is essential because the unreacted RITC was not dialyzed out from the RITC tagged to HSA. The two-component fitting leads to τ_D of 383 μs for the (tagged) HSA. The residuals for the fits are shown in Figure S1 (Supplementary Information). The τ_D of 383 μs for HSA corresponds to a hydrodynamic radius of 3.2 nm, which is in very good agreement with the reported value of 3.3-4.1 nm.[45,46]

The FCS autocorrelation curves were recorded for the RITC tagged HSA with an increase in the concentration of SDS and Figure 2A shows some representative examples. These autocorrelation curves were analysed using a two-component diffusion model (equation 3) with one component corresponding to unreacted RITC (with HSA) and the second being HSA tagged RITC. Table 1 lists the fitting parameters and the fitting residuals for three representative plots are shown in Figure S2 (Supplementary Information). However, it must be pointed out that the diffusion time the τ_{D1} (Column 2 of Table 1) corresponds to the average diffusion behaviour of the unreacted RITC and will comprise of individual components of free dye, and its interaction with SDS and protein through non-specific aggregations. It can be seen from Table 1 that an increase in the SDS concentration (0-400 mM) leads to an increase in diffusion time of both the unreacted RITC (from 56-293 μs) and RITC tagged HSA (383-1002 μs).

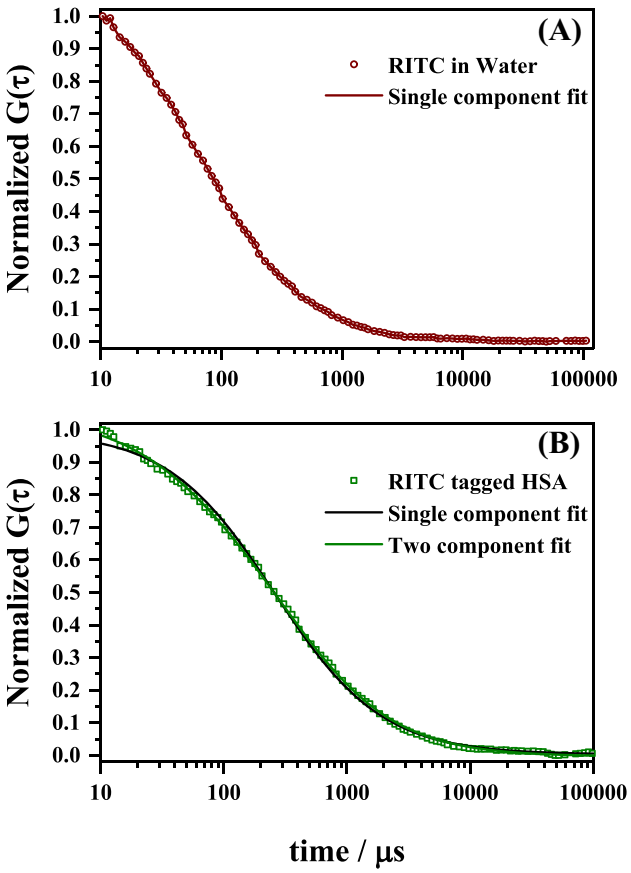

Figure 1. Normalized FCS autocorrelation curve for (A) RITC in water (red open circles) and the red solid line is the single component (equation 2) fit to the data points. (B) RITC tagged HSA (green open squares) and the black and the green solid lines are single (equation 2) and two (equation 3) component fits to the data points. Notice that for RITC tagged HSA, a two-component (equation 3) analysis fits the data more accurately, and are visible in the early part of the autocorrelation curve. The residuals for the single and two-component fits are given in Figure S1 (Supplementary Information).

In order to understand the trends in the variation of τ_D of HSA in the presence of SDS, two sets of control experiments were also carried out. In the first set of control experiments, the Rh6G dye was used as a fluorescent tracer for monitoring the aggregation of SDS in the concentration range of 0-400 mM and Figure 2B depicts some representative examples. The FCS autocorrelation curves, in this case, were analysed using two-component model, one each

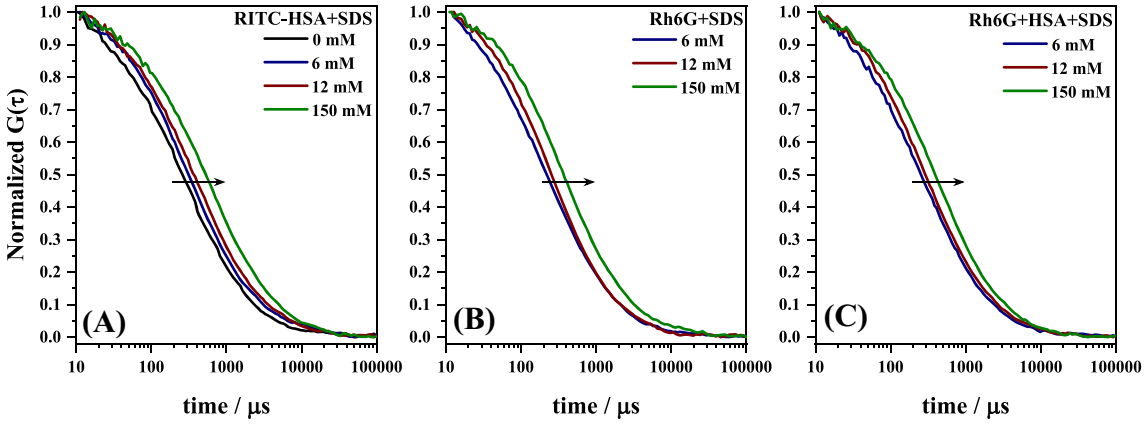

Figure 2. Normalized FCS autocorrelation curves at various SDS concentrations for (A) RITC tagged HSA, (B) Rh6G dye, and (C) mixture of HSA and Rh6G. The SDS concentrations used were 6 mM (below CMC), 8 mM (just above CMC) and 150 mM (much higher than CMC). In all the three cases the autocorrelation curve was fitted to a two-component diffusion model (equation 3). Notice the increase in the diffusion time (τ_D) with an increase in SDS concentration. The residuals for the single and two-component fits are given in Figure S2 (see the SI).

Table 1. Autocorrelation coefficients (G_1 and G_2) and diffusion times (τ_D, τ_{D1} and τ_{D2} in μs) for RITC tagged HSA, mixture of Rh6G dye and HSA, and Rh6G dye as a function of SDS concentration. The autocorrelation curves were analysed using a two-component model for RITC tagged HSA and mixture of Rh6G dye and HSA, while a single component model was used for Rh6G dye.

	RITC tagged HSA				Rh6G					Rh6G + HSA (25 nM)				
[SDS]	G_1	τ_{D1}	G_1	τ_{D2}	τ_D	G_1	τ_{D1}	G_2	τ_{D2}	τ_D	G_1	τ_{D1}	G_2	τ_{D2}
0	0.30	56	0.74	383	56	-	-	-	-	63	0.57	56	0.58	72
1	0.31	75	0.72	445	59	0.46	56	0.68	70	64	0.58	56	0.65	80
2	0.30	85	0.73	482	68	0.50	56	0.56	88	69	0.40	56	0.70	279
4	0.32	115	0.72	522	176	0.49	56	0.60	214	114	0.29	56	0.77	306
6	0.30	135	0.74	590	213	0.35	56	0.72	245	249	0.12	56	0.91	312
8	0.30	150	0.74	619	240	0.14	56	0.90	282	270	0.13	56	0.92	316
10	0.29	175	0.72	620	242	0.12	56	0.94	285	272	0.11	56	0.92	335
12	0.27	185	0.72	626	247	0.08	56	0.97	286	281	0.10	56	0.92	331
16	0.30	190	0.73	630	250	0.10	56	0.98	285	283	-	-	-	-
20	0.28	200	0.72	687	262	0.04	56	0.99	301	288	-	-	-	-
25	0.29	220	0.73	739	267	-	-	-	-	288	-	-	-	-
50	0.28	235	0.72	837	275	-	-	-	-	328	-	-	-	-
100	0.27	240	0.72	905	285	-	-	-	-	362	-	-	-	-
150	0.28	250	0.73	962	299	-	-	-	-	394	-	-	-	-
200	0.27	275	0.72	1002	310	-	-	-	-	428	-	-	-	-
300	0.27	280	0.73	1005	317	-	-	-	-	445	-	-	-	-
400	0.27	296	0.72	1002	325	-	-	-	-	460	-	-	-	-

corresponding to the free[42] and SDS bound Rh6G dye, However, it was observed that beyond 20 mM SDS concentration free Rh6G dye does not exist in the medium (Columns 7-10, Table 1) and the Rh6G is bound to the microstructures of SDS. Therefore, a single component analysis leads to the average diffusion behaviour of the Rh6G dye in the presence of SDS, and the corresponding diffusion times are listed in Table 1 (Column 6), which is similar to unreacted RITC. The second set of control experiments involved the mixture of HSA (25 nM) with varying concentrations of SDS (0-400 mM) wherein Rh6G dye was once again used as a fluorescent tracer. The FCS autocorrelation curves analysed using two-component model indicates that beyond 12 mM concentration of SDS, free Rh6G dye is unavailable in the milieu (Columns 12-15, Table 1), therefore once again the average diffusion behaviour of Rh6G dye was estimated using a single component fitting, similar to the other two cases and the resulting diffusion time are listed in Table 1 (Column 11). The diffusion time behaviour of three sets of experiments as a function of

SDS concentration are plotted in Figure 3. In the first set of control experiments, the variation in the diffusion time of bound Rh6G against SDS concentration suggests that in the initial phase (0-2 mM SDS) represents molecular-level interaction between SDS and Rh6G and has very little influence over the diffusion time of the bound Rh6G. In the next phase, the (2-8 mM SDS) the diffusion time of the bound Rh6G increases rather rapidly to about 250 μs which represents the cooperative aggregation regime, leading to micelle formation around 8 mM of SDS, which corresponds critical micellar concentration (CMC) of SDS. After CMC only one diffusing component is observed in the set. The diffusion time remains almost constant up to 20 mM concentration of SDS and thereafter increases very gradually to about 300 μs, which can be attributed to the micellar growth phase (20-400 mM). The higher τ_D of Rh6G in the presence of the HSA can be attributed to the averaging effect of two types of bound Rh6G, which include Rh6G bound to SDS aggregates and HSA-SDS aggregates. On the other hand, it was observed that the diffusion time of unreacted RITC and Rh6G in the presence of HSA show very similar behaviour, however, there are differences in the diffusion times, which can be attributed to the specific interaction between the RITC and Rh6G with SDS-HSA aggregates, which could be different due to differences in their molecular structure.

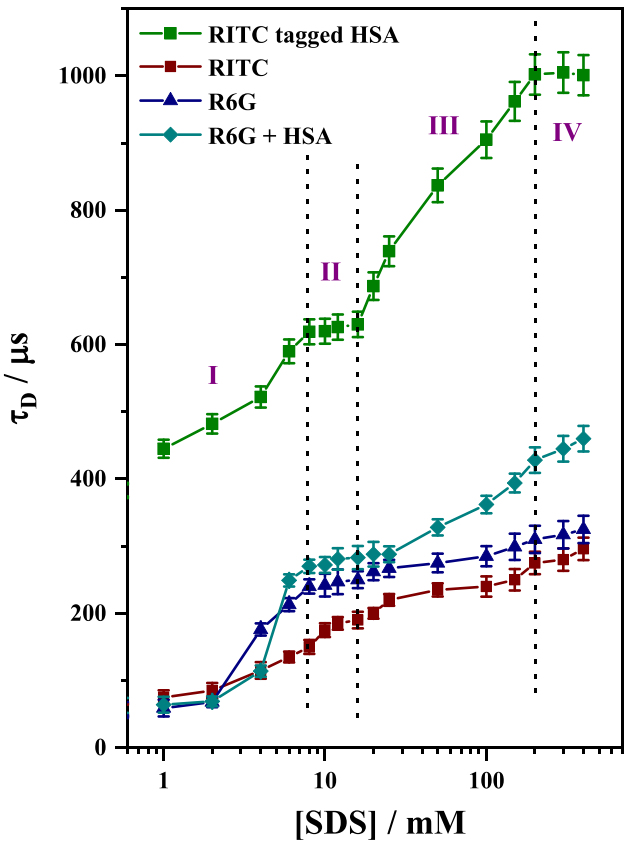

Figure 3. Plots of average diffusion times of (i) unreacted RITC in the presence of HSA 25 nM (circles), (ii) Rh6G dye (triangles), (iii) Rh6G in the presence of HSA 25 nM (diamonds) and (iv) RITC tagged HSA (squares) as a function of SDS concentration. The error bars represent 1σ (standard deviation) values calculated from five sets of measurements.

With the observed trends in the diffusion time as a function of SDS concentration for the two sets of control experiments analysed, it is now prudent to analyse the diffusion time of RITC tagged HSA as a function of SDS concentration, which also shown in Figure 3. In this set of experiments, since the RITC is covalently tagged to HSA, therefore, any changes are due to the diffusion behaviour of the protein. The addition of SDS (0-8 mM) to HSA increases the diffusion time from 380 μs to 590 μs (region-I), which is due to opening up of the tertiary structure of the HSA. Interestingly, the diffusion time remains constant in the 8-16 mM SDS, which can be interpreted as non-specific SDS aggregation (micelle formation) (region-II). The 16-200 mM SDS concentration region shows the most dramatic change in the diffusion time (630-1000 μs) which is due to the opening up of the secondary structure of the HSA (region-III). Beyond 200 mM SDS the diffusion time remains constant, which suggests that further addition of SDS does not affect the structure of the protein (region-IV). Therefore, it is reasonable to assume that SDS aggregates around the secondary structure of the protein, leading to the formation of a necklace-bead model of protein-surfactant aggregate. The interaction of SDS with HSA leads to an increase in the diffusion time of 383 μs for the free protein to 1000 μs for the SDS aggregated protein. This increase in the diffusion time translates to an increase in the hydrodynamic radius by about 2.6 times. Earlier reported dynamic light scattering (DLS) studies indicate an increase in hydrodynamic radius of about 2.2 times.[47] The DLS measurements are more likely to be influenced by the presence of external particles in comparison to FCS measurements, the estimated increase of hydrodynamic radius of HSA by a factor of 2.6 is therefore likely to be more reliable. The FCS experiments on the interaction of SDS with homologous protein bovine serum albumin (BSA) leads to qualitatively similar results.[48] However, the increase in the hydrodynamics radius of BSA due to interaction with SDS was reported to be a factor of 1.6, substantially less than in the present case. The diffusion behaviour of untagged free dye in the solution matches with that of control set 1 of the experiment indicating the interaction of the free dye with the micelles formed. A slight decrease in

the amount of free dye in the solution is observed, this may be due to the binding of some free dye to HSA-SDS aggregates.

4. Conclusions

Surfactant induced denaturation of HSA was monitored by measuring the translational diffusion properties of the protein on near single molecular level. Two sets of control experiments were performed using rhodamine-6G as a fluorescent tracer to evaluate the aggregation behaviour of SDS and SDS in the presence of 25 nM HSA. These experiments provide a reasonable foundation to understand the unfolding of HSA in the presence of SDS. The initial binding of SDS (0-8 mM) leads to the opening of the tertiary structure wherein the diffusion time increases from $\sim$380 μs to 590 μs. This is followed by a plateau region with 8-16 mM SDS which is due to non-specific aggregation of SDS around HSA, without affecting the structure of HSA. The opening of the secondary structure of the protein was observed with 16-200 mM SDS concentration. Finally, beyond 200 mM SDS concentration, the diffusion time saturates due to the formation of protein-bound micelles. The total increase in the diffusion time for the SDS concentration ranging from 0-400 mM translates to increase in the hydrodynamic radius of HSA by a factor of 2.6.

Supplementary Information (SI)

Figures S1-S2 depicting normalized FCS autocorrelation curves, and their fits with single and two components fits along with the residuals are available at www.ias.ac.in/chemsci.

Acknowledgements

Authors wish to thank Prof. Sudipta Maiti for his help in setting up the FCS instrument as part of the first FCS workshop held at TIFR in the year 2009. The FCS instrument was procured as part of the Department of Information Technology Govt. of India sponsored research project entitled Construction and multi-site commissioning of multiple fluorescence correlation spectrometers [Project No. 12(4)/2007-PDD]. VS gratefully acknowledges CSIR for fellowship.

References

1. Otzen D 2011 Protein–surfactant interactions: a tale of many states *Biochim. Biophys. Act. (BBA)* **1814** 562
2. Cooper A and Kennedy M W 2010 Biofoams and natural protein surfactants *Biophys. Chem.* **151** 96
3. Vasilescu M and Angelescu D 1999 Interactions of globular proteins with surfactants studied with fluorescence probe methods *Langmuir* **15** 2635
4. Gelamo E L and Tabak M 2000 Spectroscopic studies on the interaction of bovine (BSA) and human (HSA) serum albumins with ionic surfactants *Spectrochim. Acta Part A* **56** 2255
5. Vlasova I M and Saletsky A M 2011 Polarized fluorescence in the study of rotational diffusion of human albumin during denaturation under the action of SDS *Moscow Univ. Phys. Bull.* **1** 58
6. Vlasova I M and Saletsky A M 2009 Fluorescence of tryptophan in the denaturation of human serum albumin under the action of sodium dodecyl sulfate *Russ. J. Phys. Chem. B* **3** 976
7. Anand U, Jash C and Mukherjee S 2010 Spectroscopic probing of the microenvironment in a protein-surfactant assembly *J. Phys. Chem. B* **114** 15839
8. Hazra P, Chakrabarty D, Chakraborty A and Sarkar N 2004 Probing protein–surfactant interaction by steady state and time-resolved fluorescence spectroscopy *Biochem. Biophys. Res. Commun*. **314** 543
9. Turro N J, Lei X G, Ananthapadmanabhan K P and Aronson M 1995 Spectroscopic probe analysis of protein-surfactant interactions: the BSA/SDS system *Langmuir* **11** 2525
10. Shweitzer B, Zanette D and Itri R 2004 Bovine serum albumin (BSA) plays a role in the size of SDS micelle-like aggregates at the saturation binding: the ionic strength effect *J. Coll. Inter. Sci.* **277** 285
11. Santos S F, Zanette D, Fischer H and Itri R 2003 A systematic study of bovine serum albumin (BSA) and sodium dodecyl sulfate (SDS) interactions by surface tension and small angle X-ray scattering *J. Colloid Interface Sci.* **262** 400
12. Moriyama Y, Ohta D, Hachiya K, Mitsui Y and Takeda K 1996 Fluorescence behavior of tryptophan residues of bovine and human serum albumins in ionic surfactant solutions: a comparative study of the two and one tryptophan(s) of bovine and human albumins *J. Prot. Chem.* **15** 265
13. Moriyama Y and Takeda K 1999 Re-formation of the helical structure of human serum albumin by the addition of small amounts of sodium dodecyl sulfate after the disruption of the structure by urea. A comparison with bovine serum albumin *Langmuir* **15** 2003
14. Moriyama Y, Kanasaka and Takeda K 2003 Protective effect of small amounts of sodium dodecyl sulfate on the helical structure of bovine serum albumin in thermal denaturation *J. Colloid Interface Sci.* **257** 41
15. Chatterjee S and Mukherjee T K 2016 Insights into the morphology of human serum albumin and sodium dodecyl sulfate complex: a spectroscopic and microscopic approach *J. Colloid Interface Sci*. **478** 29
16. Mukherjee T K, Lahiri P and Datta A 2007 2-(2′-Pyridyl)benzimidazole as a fluorescent probe for monitoring protein–surfactant interaction *Chem. Phys. Lett*. **438** 218
17. Reynolds J A and Tanford 1970 Binding of dodecyl sulfate to proteins at high binding ratios. Possible

implications for the state of proteins in biological membranes *Proc. Natl. Acad. Sci. U.S.A.* **66** 1002
18. Allen G 1974 The binding of sodium dodecyl sulphate to bovine serum albumin at high binding ratios *Biochemistry J.* **137** 575
19. Laurie O and Oakes J 1975 Protein-surfactant interactions. Spin label study of interactions between bovine serum albumin (BSA) and sodium dodecyl sulphate (SDS) *J. Chem. Soc. Faraday Trans. 1* **71** 1324
20. Oakes J 1974 Protein-surfactant interactions. Nuclear magnetic resonance and binding isotherm studies of interactions between bovine serum albumin and sodium dodecyl sulphate *J. Chem. Soc. Faraday Trans. 1* **70** 2200
21. Shinagawa S, Sato M, Kameyama K and Takagi T 1994 Effect of salt concentration on the structure of protein-sodium dodecyl sulfate complexes revealed by small-angle X-ray scattering *Langmuir* **10** 1690
22. Santra M K, Banerjee A, Rahaman O and Panda 2005 Unfolding pathways of human serum albumin: evidence for sequential unfolding and folding of its three domains *Int. J. Biol. Macromol.* **37** 200
23. He X M and Carter D C 1992 Atomic structure and chemistry of human serum albumin *Nature* **358** 209
24. Dugaiczyk A, Law S W and Dennison O E 1982 Nucleotide sequence and the encoded amino acids of human serum albumin mRNA *Proc. Natl. Acad. Sci. U.S.A.* **79** 71
25. Green A M and Abelt C J 2015 Dual-sensor fluorescent probes of surfactant-induced unfolding of human serum albumin *J. Phys. Chem. B* **119** 3912
26. Yadav R, Sengupta B and Sen P 2014 Conformational fluctuation dynamics of domain I of human serum albumin in the course of chemically and thermally induced unfolding using fluorescence correlation spectroscopy *J. Phys. Chem. B* **118** 5428
27. Magde D, Elson E and Webb W W 1972 Thermodynamic fluctuations in a reacting system-measurement by fluorescence correlation spectroscopy *Phys. Rev. Lett.* **29** 705
28. Elson E L and Magde D 1974 Fluorescence correlation spectroscopy. I. Conceptual basis and theory *Biopolymers* **13** 1
29. Widengren J, Dapprich J and Rigler R 1997 Fast interactions between Rh6G and dGTP in water studied by fluorescence correlation spectroscopy *Chem. Phys.* **216** 417
30. Haustein E and Schwille P 2007 Fluorescence correlation spectroscopy: novel variations of an established technique *Annu. Rev. Biophys. Biomol. Struct.* **36** 151
31. Wöll D 2014 Fluorescence correlation spectroscopy in polymer science *RSC Adv.* **4** 2447
32. Rathgeber S, Beauvisage H J, Chevreau H, Willenbacher N and Oelschlaeger C 2009 Microrheology with fluorescence correlation spectroscopy *Langmuir* **25** 6368
33. Kim S 2003 Intracellular applications of fluorescence correlation spectroscopy: prospects for neuroscience *Curr. Opin. Neurobiol.* **13** 583
34. Wachsmuth M, Waldeck W and Langowski J 2000 Counting nucleosomes in living cells with a combination of fluorescence correlation spectroscopy and confocal imaging *J. Mol. Biol.* **298** 677
35. Sengupta P, Balaji J and Maiti S 2002 Measuring diffusion in cell membranes by fluorescence correlation spectroscopy *Methods* **27** 374
36. Sengupta P, Garai K, Balaji J, Periyasami N and Maiti S 2003 Measuring size distribution in highly heterogeneous systems with fluorescence correlation spectroscopy *Biophys. J.* **84** 1977
37. Al-soufi W, Novo M, Felekyan S and Seidel C A M 2005 Fluorescence correlation spectroscopy, a tool to investigate supramolecular dynamics: inclusion complexes of pyronines with cyclodextrin *J. Am. Chem. Soc.* **109** 8775
38. Al-Soufi W, Reija B, Felekyan S, Seidel C M and Novo M 2008 Dynamics of supramolecular association monitored by fluorescence correlation spectroscopy *Chem. Phys. Chem.* **9** 1819
39. Sherman E, Itkin A, Kuttner Y Y, Rhoades E, Amir D, Haas E and Haran G 2008 Using fluorescence correlation spectroscopy to study conformational changes in denatured proteins *Biophys. J.* **94** 4819
40. Sen Mojumdar S, Chowdhury R, Chattoraj S and Bhattacharyya K 2012 *J. Phys. Chem. B* **116** 12189
41. Sasmal D K, Mondal T, Sen Mojumdar S, Choudhury A, Banerjee R and Bhattacharyya K 2011 An FCS study of unfolding and refolding of CPM-labeled human serum albumin: role of ionic liquid *J. Phys. Chem. B* **115** 13075
42. Ghosh S, Adhikari A, Sen Mojumdar S and Bhattacharyya K 2010 A fluorescence correlation spectroscopy study of the diffusion of an organic dye in the gel phase and fluid phase of a single lipid vesicle *J. Phys. Chem. B* **114** 5736
43. Rigler R and Elson E S 2000 *Fluorescence Correlation Spectroscopy: Theory and Applications Springer Series in Chemical Physics* vol. 65 (Berlin: Springer Verlag)
44. Magde D, Elson E L and Webb W W 1974 Fluorescence correlation spectroscopy. I. Conceptual basis and theory. Fluorescence correlation spectroscopy conceptual basis and theory. II *Biopolymers* **13** 29
45. Jachimska B, Wasilewska M and Adamczyk Z 2008 Characterization of globular protein solutions by dynamic light scattering, electrophoretic mobility, and viscosity measurements *Langmuir* **24** 6866
46. Leggio C, Galantini L, Konarev P V and Pavel N V 2009 Urea-induced denaturation process on defatted human serum albumin and in the presence of palmitic acid *J. Phys. Chem. B* **113** 12590
47. Anand U, Ray S, Ghosh S, Banerjee R and Mukherjee S 2015 Structural aspects of a protein–surfactant assembly: native and reduced states of human serum albumin *Protein J.* **34** 147
48. Zhang X, Poniewierski A, Hou S, Sozanski K, Wisniewska A, Wieczorek S A, Kalwarczyk T, Sun L and Hołyst R 2015 Tracking structural transitions of bovine serum albumin in surfactant solutions by fluorescence correlation spectroscopy and fluorescence lifetime analysis *Soft Matter* **11** 2512